Velocity-dependent collision rates from light-induced drift experiments: C_2H_4–noble-gas mixtures

G. J. van der Meer, J. Smeets, E. R. Eliel, P. L. Chapovsky,* and L. J. F. Hermans
Huygens Laboratory, Leiden University, P.O. Box 9504, 2300 RA Leiden, The Netherlands
(Received 24 July 1992)

Light-induced drift arises in a binary mixture when velocity-selective optical excitation is combined with a state-dependent kinetic collision frequency (or cross section). This phenomenon is studied experimentally for rovibrationally excited C_2H_4 immersed in the atomic buffer gases Ne, Ar, Kr, or Xe at temperatures between 275 and 500 K. In several cases, the laser-frequency dependence of the drift is observed to be anomalous and to change dramatically with temperature. This means that the relative change in collision frequency upon excitation depends strongly on velocity. To evaluate the data, an analytic model description is presented and applied to the experimental data. It is found that for each particular buffer gas, all data are well described with a relative difference in collision rate depending on a single parameter only, i.e., the average relative velocity. This dependence is found to be different for the various noble gases. This suggests that the attractive part of the interaction potential is crucial for the occurrence of anomalous light-induced drift.

PACS number(s): 42.50.Vk, 33.80.−b

I. INTRODUCTION

Light-induced drift (LID) is a phenomenon at the interface between kinetic theory and laser spectroscopy [1–4]. It arises in a two-component gas consisting of light-absorbing particles immersed in a buffer gas, when velocity-selective optical excitation is combined with a difference in kinetic collision frequency between excited- and ground-state particles with respect to the buffer gas. This yields a drift of the absorbing species through the buffer gas. In most experiments so far, the light-induced drift velocity $v_{\rm dr}$ could be well described by standard theory [5] (based on the strong-collision model). For δ-peak excitation of the velocity group around v_{xL} by a light beam propagating in the **x** direction, one has

$$v_{\rm dr}=-\frac{\Delta\nu}{\nu}\frac{n_e}{n_a}v_{xL}\ . \tag{1}$$

Here, $\Delta\nu/\nu\equiv(\nu_e-\nu_g)/\nu_g$ is the relative change upon excitation in collision frequency and n_e/n_a is the fraction of excited particles which have not yet suffered a velocity-randomizing collision (more precisely, $n_e v_{xL}$ is the steady-state flux of excited particles). When a laser with low, constant power is scanned through the absorption profile of the gas, n_e/n_a follows the Maxwell velocity distribution as a function of detuning $\Omega=kv_{xL}$. Therefore, if $\Delta\nu/\nu$ is independent of velocity, $v_{\rm dr}$ has a dispersionlike shape as a function of the laser detuning.

For most molecular species studied so far, the drift velocity indeed had this simple dispersionlike shape. This is known as standard LID. In recent experiments on C_2H_4 immersed in Kr, however, a more complex dependence of the drift velocity on the laser detuning was observed with an additional zero crossing at either side of line center [6]. Henceforth, we will refer to such a complex detuning dependence as anomalous LID.

Ethylene (C_2H_4) is a planar, asymmetric top molecule. Hence its rotational states are described by (J,K_a,K_c), with J the rotational quantum number and K_a its projection along the C=C bond. The quantum number K_c can only take the values $J-K_a$ and $J-K_a+1$ [7]. The molecule can be excited with a CO_2 laser into its ν_7 fundamental vibrational mode (out-of-plane bending mode).

Anomalous LID was first observed for the $(4,1,3)\rightarrow\nu_7(5,0,5)$ transition of C_2H_4 in Kr as a buffer gas [6]. Subsequently, the system C_2H_4-Kr was studied for a large number of rotational sublevels in the same ν_7 mode and anomalous features were observed for a whole series of rovibrational transitions [8]. In the same paper, a strong dependence of $\Delta\nu/\nu$ on the rotational sublevels was reported also. A model to describe the results was proposed [8], in which the collision rates were assumed to depend on both the vibrational and the rotational state of the molecule. In the model [8], it was found that the formula for the drift velocity is quite similar to the simple two-level expression. Only, $\Delta\nu/\nu$ has to be interpreted as an effective relative change in collision frequency upon excitation, $(\Delta\nu/\nu)_{\rm eff}$, which now consists of two contributions:

$$\left[\frac{\Delta\nu}{\nu}\right]_{\rm eff}=\left[\frac{\Delta\nu}{\nu}\right]_{\rm vib}+\frac{\nu}{\nu+\nu_{\rm res}}\left[\frac{\Delta\nu}{\nu}\right]_{\rm rot}\ . \tag{2}$$

Here, the subscripts vib and rot denote the vibrational and a rotational part of $\Delta\nu/\nu$, respectively. The factor $\nu/(\nu+\nu_{\rm res})$ takes into account that rotational-state-changing collisions, which occur on roughly the same time scale as velocity-randomizing collisions, can reduce the rotational contribution to $\Delta\nu/\nu$. Here, $\nu_{\rm res}$ is the rate of collisions which establish an equilibrium distribution over the rotational states, but *not* over the velocity, e.g., resonant collisions. These collisions tend to reduce the

rotational part in $(\Delta\nu/\nu)_{\text{eff}}$ by scrambling the rotational-state distribution before the velocity is randomized. Furthermore, ν is the total rate of transport collisions (velocity-changing collisions) containing both an inelastic and an elastic contribution [8]. In the derivation of Eq. (2), it was assumed that, first, the homogeneous linewidth is small compared to the Doppler width and, second, all factors appearing in Eq. (2) have only a small velocity dependence. Then anomalous LID arises when two conditions are met: first, the rotational and the vibrational parts in Eq. (2) are of roughly equal magnitude but of opposite sign, while their velocity dependence differs. Second, when the laser is tuned through the absorption profile—and thus the $\mathbf{x}$ velocity of the excited molecules is varied—the average relative velocity of the molecule and the buffer gas particles must vary substantially [8,9]. The first condition seems to be met for C_2H_4-Kr since $(\Delta\nu/\nu)_{\text{vib}}$ is small [8]. Hence, it should be relatively easy to find rotational sublevels such that the vibrational term is offset by the rotational term. The second condition is also met since Kr is a heavy buffer gas. Thus, the average relative velocity is determined mainly by the velocity of the lighter C_2H_4 molecule.

In this paper we present an analytic description for LID with transport collision rates having an arbitrary velocity dependence. Then we can accurately describe the laser detuning dependence of anomalous LID. Furthermore, we employ the model to describe the drift as a function of the average relative velocity rather than as a function of detuning, or v_{xL}. Experimentally, two independent approaches are used to vary this average relative velocity between the ethylene molecule and the buffer gas atom. On the one hand, the temperature of the gas is varied; on the other hand, experiments are performed using buffer gases with a different mass. We will elucidate both aspects. The variation of the average relative velocity by changing the buffer gas will only be discussed qualitatively because the interaction potential varies significantly with the buffer gas.

II. MODEL FOR VELOCITY-DEPENDENT COLLISION RATES

Recently, analytical models of LID with velocity-dependent transport collision rates have been put forward [9,10]. In this section we give an intuitive derivation, suitable for a description of the dependence of $(\Delta\nu/\nu)_{\text{eff}}$ on the average relative velocity. In Ref. [8], it was pointed out that, although molecules are multilevel particles, the expression for the drift velocity is identical to that of a two-level particle if $\Delta\nu/\nu$ is interpreted as an effective relative difference in collision rate, $(\Delta\nu/\nu)_{\text{eff}}$. Therefore, we will restrict ourselves to a two-level description here also. In the end, the expression for the velocity-dependent $\Delta\nu/\nu$ will be identified with $(\Delta\nu/\nu)_{\text{eff}}$.

Consider two-level particles, infinitely diluted in a buffer gas. Suppose that a laser gives rise to an excitation probability $p(\mathbf{v})d\mathbf{v}$ per unit time for molecules with a velocity between $\mathbf{v}$ and $\mathbf{v}+d\mathbf{v}$. The excited-state velocity distribution is given by

$$n_e(\mathbf{v})=n_e^0 W(\mathbf{v})+f_e(\mathbf{v}) ,$$

where $n_e^0 W(\mathbf{v})$ denotes the equilibrium (Maxwell) distribution and $f_e(\mathbf{v})$ is the deviation from equilibrium caused by the laser. Similarly, the ground-state distribution is

$$n_g(\mathbf{v})=n_g^0 W(\mathbf{v})+f_g(\mathbf{v}) .$$

Integration of the distributions over velocity space yields the corresponding densities $n_j=\int d\mathbf{v}\, n_j(\mathbf{v})$ (with $j=e,g$), such that $n_a=n_e+n_g$ is the total number density of absorbing particles. The laser excitation produces two opposing fluxes, which can be calculated purely from the nonequilibrium parts $f_j(\mathbf{v})$ (with $j=e,g$). LID occurs when $f_g(\mathbf{v})+f_e(\mathbf{v})\neq 0$, i.e., when the ground and excited particles have a different velocity-relaxation rate to equilibrium. Note that in the absence of collisional relaxation, $f_g(\mathbf{v})+f_e(\mathbf{v})=0$.

We will assume that under stationary conditions in an open tube, the relaxation of the nonequilibrium parts of velocity distributions in the excited (e) and in the ground state (g) is described by the following equations:

$$-\nu_e(\mathbf{v})f_e(\mathbf{v})+n_a p(\mathbf{v})=0 , \tag{3}$$

$$-\nu_g(\mathbf{v})f_g(\mathbf{v})-n_a p(\mathbf{v})=0 . \tag{4}$$

Here, $\nu_j(\mathbf{v})$ is the relaxation rate to an equilibrium velocity distribution for particles in state j by collisions with the buffer gas. From a comparison with the full kinetic equation [8], we see that the effective relaxation rate has replaced the collision integral. In Ref. [10], the validity of these equations is proven with the help of Green functions. As can be seen from Eqs. (3) and (4), $f_j(\mathbf{v})$ (with $j=e,g$) is determined by the excitation probability $p(\mathbf{v})$, which in the low-saturation limit is

$$p(\mathbf{v})\propto \frac{W(\mathbf{v})}{\Gamma^2+(\Omega-\mathbf{k}\cdot\mathbf{v})^2} . \tag{5}$$

Here, Γ is the homogeneous linewidth [half width at half maximum (HWHM)] of the transition and Ω is the laser detuning relative to the absorption line center.

The drift velocity is easily calculated from Eqs. (3) and (4):

$$\begin{aligned}\mathbf{v}_{\text{dr}}&=\frac{1}{n_a}\int d\mathbf{v}\,\mathbf{v}[f_e(\mathbf{v})+f_g(\mathbf{v})]\\&=\int d\mathbf{v}\,\mathbf{v}p(\mathbf{v})\left[\frac{1}{\nu_e(\mathbf{v})}-\frac{1}{\nu_g(\mathbf{v})}\right] .\end{aligned} \tag{6}$$

Since the drift velocity in molecular systems is small, it is not measured directly. Instead, the concentration difference along a closed tube is recorded in the steady state. Under these conditions, the LID flux is balanced by a diffusion flux, i.e.,

$$n_a\mathbf{v}_{\text{dr}}=D_{ab}(n_a+n_b)\nabla x_a , \tag{7}$$

with n_b the number density of the buffer gas and $x_a=n_a/(n_a+n_b)$ is the mole fraction of the absorbing species. The binary diffusion coefficient D_{ab} is written in terms of the (ensemble-averaged) collision rate ν through the relation $D_{ab}=\frac{1}{2}v_0^2/\nu$, where $v_0=\sqrt{2k_BT/m_a}$.

When Eqs. (6) and (7) are combined, we obtain an expression for the concentration gradient along the tube

$$\tfrac{1}{2}v_0^2(n_a+n_b)\nabla x_a=-n_a\int d\mathbf{v}\,\mathbf{v}\left[\frac{\nu_e(\mathbf{v})-\nu_g(\mathbf{v})}{\nu_e(\mathbf{v})}\right]p(\mathbf{v})\ , \tag{8}$$

where we have used that

$$[\nu_e(\mathbf{v})-\nu_g(\mathbf{v})]/\nu_e(\mathbf{v})\ll 1\ .$$

The quantity

$$[\nu_e(\mathbf{v})-\nu_g(\mathbf{v})]/\nu_e(\mathbf{v})$$

in Eq. (8) can be replaced by $(\Delta\nu/\nu)_{\text{eff}}$ when the procedure of Ref. [8] for multilevel particles is followed. In Ref. [8], the integral on the right-hand side (rhs) of Eq. (8) was evaluated under the assumption that the variations in $(\Delta\nu/\nu)_{\text{eff}}$ are small over the homogeneous linewidth Γ. In this paper, a less restrictive approach will be used, such that

$$[\nu_e(\mathbf{v})-\nu_g(\mathbf{v})]/\nu_e(\mathbf{v})\ ,$$

or equivalently, $(\Delta\nu/\nu)_{\text{eff}}$, can have an arbitrary velocity dependence.

First, the traditional assumption is made that only the **x**-velocity component is affected by the laser excitation, while the distribution over the orthogonal velocity components remains in equilibrium. Then we can average the rhs of Eq. (8) over these velocities. Next, we try to expand

$$\langle[\nu_e(\mathbf{v})-\nu_g(\mathbf{v})]/\nu_e(\mathbf{v})\rangle\equiv(\Delta\nu/\nu)_{\text{eff}}$$

with respect to some appropriate parameter. To this end, we realize that collision rates for a particular system depend on the average relative velocity between the two collision partners rather than on their absolute velocities. Consequently, also $(\Delta\nu/\nu)_{\text{eff}}$ is expected to vary with this parameter [8,9]. For a given **x** component of the velocity, the average relative velocity is determined by the gas temperature T. Let us suppose that a light-absorbing particle has velocity **v** and a buffer gas particle has velocity **u** (both in the lab frame). All velocity components of **v** and **u** have Gaussian probabilities, except v_x. The relative velocity between the active particle and the buffer gas atom equals $\mathbf{v}-\mathbf{u}$. Then the root-mean-square relative velocity $v_{\text{rms}}\equiv\sqrt{\langle(\mathbf{v}-\mathbf{u})^2\rangle}$ can be calculated by taking the ensemble average over **u** and the velocity components v_y and v_z, i.e.,

$$v_{\text{rms}}^2=\int dv_y\int dv_z\int du_x\int du_y\int du_z W_a(v_y)W_a(v_z)W_b(u_x)W_b(u_y)W_b(u_z)(\mathbf{v}-\mathbf{u})\cdot(\mathbf{v}-\mathbf{u})\ . \tag{9}$$

Here, $W_j(w_i)$ is a normalized Maxwellian velocity distribution over velocity w_i of particles j. Equation (9) yields

$$v_{\text{rms}}=\left[v_x^2+k_BT\left[\frac{2}{m_a}+\frac{3}{m_b}\right]\right]^{1/2}\ , \tag{10}$$

where m_a and m_b are the mass of the active particle and buffer gas atom, respectively.

For the expansion of $(\Delta\nu/\nu)_{\text{eff}}$, we therefore make the ansatz

$$\left[\frac{\Delta\nu}{\nu}\right]_{\text{eff}}=\sum_{m=0}^{\infty}\Delta_m\left[\frac{v_0}{v_{\text{rms}}}\right]^{2m}$$
$$=\Delta_0+\Delta_1\left[\frac{m_av_x^2}{2k_BT}+1+\frac{3m_a}{2m_b}\right]^{-1}+\cdots\ . \tag{11}$$

Thus, we expand in terms of Lorentzian-type functions of v_x. In the expansion, only even powers of v_x arise, since in the lab frame, $v_j(v_x)$ is independent of the sign of v_x. For large detuning, and thus for large rms relative velocity, only the velocity-independent Δ_0 term is important. This is reasonable, because for large relative velocities, the repulsive part of the intermolecular potential dominates, emphasizing the hard-sphere character [11]. In the experimental section, we will show that the series can be truncated after the second term, i.e., $(v_0/v_{\text{rms}})^2$. This already suffices for an accurate description of anomalous LID.

Substitution of Eq. (11) in Eq. (8) in combination with integration over the velocity components v_y and v_z yields

$$\tfrac{1}{2}v_0^2(n_a+n_b)\nabla_x x_a$$
$$=-n_a\int dv_x v_x p(v_x)\left[\Delta_0+\Delta_1\left[\frac{v_0}{v_{\text{rms}}}\right]^2+\cdots\right]\ . \tag{12}$$

It is convenient to introduce detuning functions $\varphi_m(\Omega)$ that are defined as

$$\int dv_x v_x p(v_x)(v_0/v_{\text{rms}})^{2m}\equiv Pv_0\varphi_m(\Omega)\ . \tag{13}$$

Here the number of photons absorbed per molecule per second, $P=\int dv_x p(v_x)$, is related to the absorbed laser power ΔP_L, through $\Delta P_L=\hbar\omega n_a P\pi R^2L$ [12], with $\hbar\omega$ the photon energy and R,L the radius and the length of the tube, respectively. The first two detuning functions $\varphi_0(\Omega)$ and $\varphi_1(\Omega)$ are

$$\varphi_0(\Omega)=\text{Re}[zw(z)]/\text{Re}[w(z)]\ , \tag{14}$$

$$\varphi_1(\Omega)=\text{Re}\left[\frac{z}{z^2-y^2}\left[w(z)-\frac{z}{y}w(y)\right]\right]\Big/\text{Re}[w(z)]\ , \tag{15}$$

where $z=(\Omega+i\Gamma)/kv_0$ is the complex detuning, $y=i\sqrt{1+3m_a/2m_b}$, and kv_0 is the Doppler width. The function $w(z)$ is related to the complex error function [13], such that $\mathrm{Re}[w(z)]$ represents a Voigt absorption profile. When $(\Delta\nu/\nu)_{\mathrm{eff}}$ is velocity independent, only the well-known function $\varphi_0(\Omega)$ [5] is important, which has a simple physical meaning: $v_0\varphi_0(\Omega)$ is the average **x** velocity that is excited at laser detuning Ω. In the δ-peak excitation limit ($\Gamma \ll kv_0$), $\varphi_0(\Omega)$ reduces to v_{xL}/v_0, while $\varphi_1(\Omega)$ equals $v_{xL}v_0/v_{\mathrm{rms}}^2$. Graphs of $\varphi_0(\Omega)$ and $\varphi_1(\Omega)$ are given in Fig. 1.

The expression for the induced concentration difference

$$\Delta x_a \equiv x_{a,\mathrm{exit}} - x_{a,\mathrm{entrance}}$$

is obtained after substituting Eq. (13) in Eq. (12) and integrating the result along the length of the tube

$$\Delta x_a = -\frac{2\Delta P_L}{(n_a+n_b)\hbar\omega v_0 \pi R^2} \sum_{m=0,1,\ldots} \Delta_m \varphi_m(\Omega) \ . \qquad (16)$$

With Eq. (16), we can describe anomalous features in LID as follows: For a realistic value of Γ/kv_0 (≈ 0.3), the functions $\varphi_0(\Omega)$ and $\varphi_1(\Omega)$ have roughly the same shape (see Fig. 1), while their amplitudes differ by approximately a factor of 2. The maximum of $\varphi_1(\Omega)$ occurs at a slightly lower detuning than that of $\varphi_0(\Omega)$. Clearly anomalous features in the concentration difference will arise when $\Delta_0 \approx -2\Delta_1$.

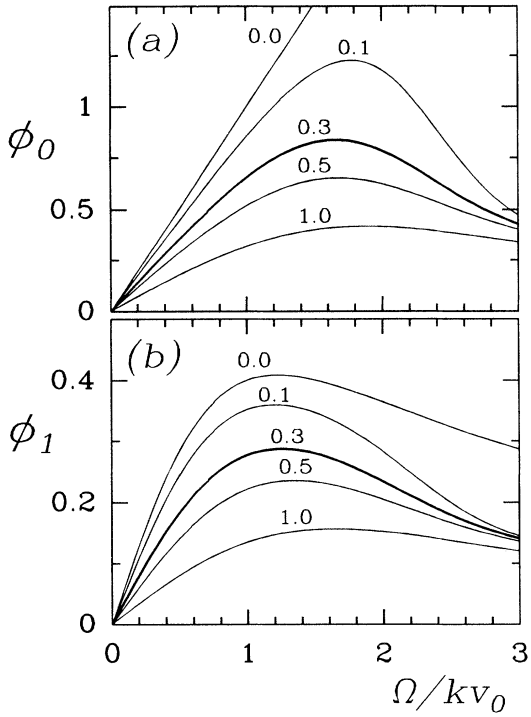

FIG. 1. The detuning functions $\varphi_0(\Omega)$ and $\varphi_1(\Omega)$, with $\Omega=kv_{xL}$, as defined in Eqs. (14) and (15) for various values of Γ/kv_0 and $y=i\sqrt{1+3m_a/2m_b}=1.2i$ (for the ethylene-krypton mass ratio). In the limit $\Gamma \ll kv_0$, φ_0 reduces to v_{xL}/v_0, while φ_1 equals $v_{xL}v_0/v_{\mathrm{rms}}^2$, with $v_{\mathrm{rms}}^2 = v_{xL}^2 + k_B T(2/m_a + 3/m_b)$.

When we fit Eq. (16) to the experimental data, we obtain explicit values for the parameters Δ_m and thus an explicit expression for the velocity-dependent effective relative difference in collision rate, $(\Delta\nu/\nu)_{\mathrm{eff}}$, through Eq. (11).

III. EXPERIMENTAL RESULTS

The setup for experiments on LID is described in Ref. [12]. In the present study, the gas is contained in a temperature-controlled quartz capillary with an inner diameter of 2 mm and a length of 30 cm. The capillary can be operated at various stable temperatures between 275 and 500 K. This is monitored by various thermocouples mounted on the capillary [14]. The light-induced difference in gas composition between the ends of the cell is monitored by two thermistors in the self-heat mode, acting as thermal conduction sensors. This provides a sensitive measurement of the concentration difference Δx_a along the tube (sensitivity ≈ 1 ppm).

Excitation of the gas is brought about using radiation of a tunable CO_2 laser, having a typical output power of 4 W and a tuning range of 260 MHz. The laser frequency is given a fixed frequency shift of 90 MHz using an extra-cavity acousto-optic modulator, which makes it almost coincident with the C_2H_4 transition under study (see below). The amount of absorbed laser power is determined using two thermopile detectors, one upstream and one downstream from the cell. In the experiment the laser frequency is slowly scanned through the absorption profile of the gas, while the resulting concentration difference Δx_a and the absorbed laser power ΔP_L are recorded on a computer.

All data presented below pertain to the $(4,1,3) \rightarrow \nu_7(5,0,5)$ transition in C_2H_4 unless stated otherwise. It has a frequency mismatch

$$\nu_{CO_2} - \nu_{\mathrm{ethylene}} = 98 \text{ MHz}$$

with respect to the center of the P(10) CO_2 line of the 10.6-μm band [15]. Various experimental crosschecks have been performed to rule out spurious thermal and pressure effects (see Ref. [6]).

A. Buffer gas Ne

The results for the buffer gas Ne are shown in Figs. 2(a) and 2(b). The absorbed laser power ΔP_L and the resulting concentration difference Δx_a are plotted for a 20-80 mixture C_2H_4-Ne at a total gas pressure of 133 Pa at 275 K (additional details are given in Table I). The concentration difference Δx_a as a function of laser detuning has a standard dispersionlike shape. Therefore, the data were first fitted with the $m=0$ term in Eq. (16) only. This yields the results shown in Fig. 2(c), where the dotted line indicates the difference between the fit and the measured curve. One then finds

$$(\Delta\nu/\nu)_{\mathrm{eff}} = (0.64 \pm 0.07)\% \ ,$$

independent of detuning, or average relative velocity v_{rms}. However, the fit can be improved significantly when the

$m=1$ term is included [the solid line in Fig. 2(c)]. This yields $\Delta_0=(0.86\pm0.05)\%$ and $\Delta_1=-(0.8\pm0.1)\%$. Though the value of Δ_1 seems rather large, the velocity dependence of $(\Delta\nu/\nu)_{\text{eff}}$ is relatively small as

$$|\Delta_1\varphi_1(\Omega)|\approx 0.3\times|\Delta_0\varphi_0(\Omega)| \ .$$

In Fig. 2(d), the result for $(\Delta\nu/\nu)_{\text{eff}}$ (with both m terms) is drawn as a function of the excited velocity class $v_{xL}=\Omega/k$. This is the variable shown on the top of Fig. 2(d). The variable along the bottom of Fig. 2(d) is the average relative velocity v_{rms}.

B. Buffer gas Ar

The results for the buffer gas Ar are shown in Fig. 3, where the absorbed laser power ΔP_L [Fig. (a)] and the resulting concentration difference Δx_a [Fig. (b)] are plotted for a 20-80 mixture C_2H_4-Ar at a total gas pressure of 133 Pa at 275 K (additional details are given in Table I). Also for Ar, Δx_a has a dispersionlike shape as a function of laser detuning. However, when Figs. 3 and 2 are compared, we see that, although the homogeneous linewidths are roughly equal for the two cases (see Table I), the extrema of Δx_a for C_2H_4 in Ar occur at larger detuning as compared to Ne. This suggests that $(\Delta\nu/\nu)_{\text{eff}}$ increases with detuning, i.e., increases with increasing relative velocity. This is made more explicit by treating the data with the procedure outlined in Secs. II and III A. As is seen in Fig. 3(c), a fit with only the $m=0$ term from Eq. (16) shows large deviations from the experiment. With both terms of Eq. (16), an excellent fit is obtained. The result for $(\Delta\nu/\nu)_{\text{eff}}$ as a function of v_{xL} and v_{rms} is drawn in Fig. 3(d).

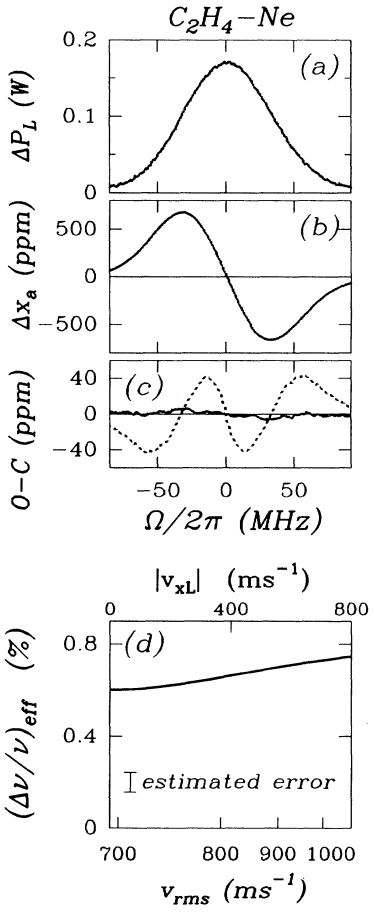

FIG. 2. Experimental results for the absorbed laser power ΔP_L (a) and the induced concentration difference Δx_a (b) as a function of laser detuning with respect to the absorption line center. These data pertain to a C_2H_4-Ne mixture at 275 K. (c) gives the difference, O−C between the observed Δx_a and the calculated fit of Eq. (16) with the $m=0$ term only (dotted line) and with both m terms (solid line). (d) shows the values of the effective relative difference in collision frequency, $(\Delta\nu/\nu)_{\text{eff}}$, which was calculated from (a) and (b), as a function of $\Omega/k=v_{xL}$ (upper axis) and of average relative velocity v_{rms} (lower axis). Relevant details are given in Table I.

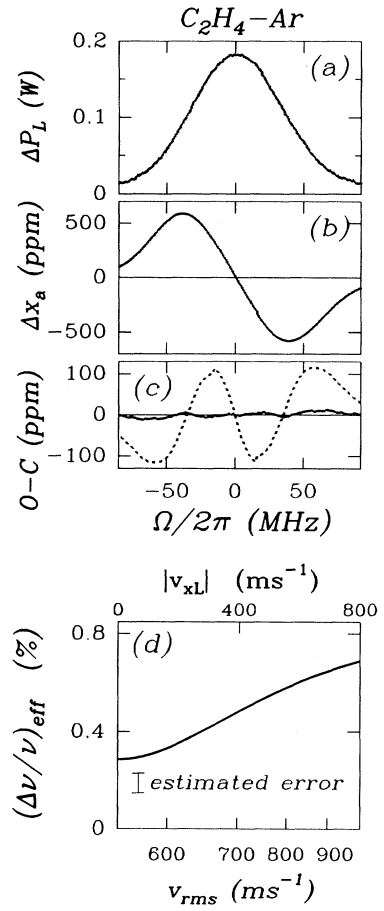

FIG. 3. Experimental results for ΔP_L and the induced concentration difference Δx_a as a function of detuning for a C_2H_4-Ar mixture at 275 K. (c) gives the difference *O-C* between the observed Δx_a and the calculated fit of Eq. (16) with the $m=0$ term (dotted line) and with both m terms (solid line). In (d) $(\Delta\nu/\nu)_{\text{eff}}$ has been calculated for various values of the detuning and of the average relative velocity. Relevant details are presented in Table I.

TABLE I. Experimental parameters relevant to Figs. 2–5. All data pertain to the (4,1,3)→ν_7(5,0,5) transition. The experiments for the buffer gases Ne and Ar were performed with a 20-80 mixture at a total gas pressure of 133 Pa, those for Kr and Xe with a 20-80 mixture at a pressure of 67 Pa. The temperature is denoted by T, the absorbed laser power at line center by ΔP_m, and the homogeneous linewidth divided by the Doppler width is Γ/kv_0. The parameters Δ_m are related to the effective relative difference in collision frequency as $(\Delta\nu/\nu)_{\text{eff}}=\sum_m \Delta_m(v_0/v_{\text{rms}})^{2m}$. The estimated error in ΔP_m, Γ/kv_0, and Δ_0 is typically 5%; in Δ_1, typically 10%.

Buffer gas	T (K)	ΔP_m (mW)	Γ/kv_0	Δ_0 (units of 10^{-2})	Δ_1 (units of 10^{-2})
Ne	275	169	0.23	0.86	−0.8
Ar	275	184	0.29	0.90	−1.3
Kr	297	45.4	0.20	0.84	−1.8
	370	21.9	0.20	0.84	−1.5
	407	15.6	0.20	0.82	−1.3
	448	10.7	0.20	0.80	−1.2
Xe	297	48.4	0.20	1.07	−2.5
	380	21.3	0.20	1.05	−2.1
	418	14.3	0.20	1.15	−2.2
	463	9.1	0.20	1.10	−1.9

C. Buffer gas Kr

The results for the buffer gas Kr are shown in Fig. 4. The absorption profiles, which are similar to those observed for the buffer gases Ne and Ar, are not shown. All relevant data are given in Table I. In Figs. 4(a)–4(d), the observed concentration difference at four different temperatures is plotted as a function of laser detuning for a 20-80 mixture C_2H_4-Kr at a total gas pressure of 67 Pa [16]. Since the population of the lower rovibrational level varies with temperature, a trivial temperature dependence of Δx_a arises. To eliminate this, the concentration difference is normalized to the absorbed laser power at line center, ΔP_m.

At two temperatures studied, we observed anomalous LID in this system: The concentration difference as a function of detuning has two extra zero crossings in addition to the one at line center. The signals are dramatically temperature dependent. With increasing temperature, the concentration difference becomes more and more dispersionlike, while the inner structure collapses.

Obviously, a fit with only the (velocity-independent) $m=0$ term cannot describe these data. The fit to the data with Eq. (16) containing both m terms is indicated by the dotted lines in Figs. 4(a)-4(d). The fit parameters are given in Table I. The values for Δ_0 are equal for all temperatures. This is consistent with the ansatz (11), where Δ_0 is the hard-sphere part of $(\Delta\nu/\nu)_{\text{eff}}$. As can be seen from Figs. 4(a)–4(d), the concentration difference is not invariant with respect to v_{xL}^2/T. Thus the coefficient Δ_1 varies with T, as is indeed found (Δ_1 is approximately proportional to T^{-1}). Furthermore, an attempt to fit the data with three terms, viz., $m=0,1,2$ in Eq. (16), did not yield a significantly better fit.

In Fig. 4(e), $(\Delta\nu/\nu)_{\text{eff}}$ as a function of v_{rms} is shown. The data for the various temperatures are seen to coincide well.

D. Buffer gas Xe

The results for the buffer gas Xe are plotted in Fig. 5. The data pertain to a 20-80 mixture C_2H_4-Xe at a total gas pressure of 67 Pa [16]. All relevant details are given in Table I.

For the buffer gas Xe, we observe anomalous LID for all temperatures. Also, here, the data show that the anomaly decreases (i.e., the magnitude of the inner extrema decreases) with increasing temperature, in line with the observations for C_2H_4 in Kr. The fit to the data is indicated by the dotted lines in Figs. 5(a)–5(d). The fit parameters given in Table I show the same trend as for Kr, viz., Δ_0 does not depend significantly on T, while Δ_1 does. In Fig. 5(e), $(\Delta\nu/\nu)_{\text{eff}}$ is shown as a function of v_{rms}. Also here, the data for the various temperatures coincide well.

E. Other transitions

For convenience, the results for $(\Delta\nu/\nu)_{\text{eff}}$ as a function of v_{rms} for the (4,1,3)→ν_7(5,0,5) transition are summarized in Fig. 6(a) for the buffer gases Ne, Ar, Kr, and Xe. Experiments were also performed on the (3,2,1)→ν_7(4,3,1) transition, which has a frequency mismatch

$$\nu_{CO_2}-\nu_{\text{ethylene}}=-111\ \text{MHz}$$

with respect to the center of the $R(22)$ CO_2 line of the 10.6-μm band [15]. The relevant experimental data are presented in Table II.

For Ne as a buffer gas, Δx_a was found to have a dispersionlike behavior. For an accurate fit, however, both m terms in Eq. (16) are required. On raising the temperature to ≈400 K, the signal changes marginally (see Table II). The result for $(\Delta\nu/\nu)_{\text{eff}}$ as a function of v_{rms} is shown in Fig. 6(b). The data for the various temperatures were found to coincide well (not shown).

TABLE II. Data for the (3,2,1)→ν_7(4,3,1) transition of ethylene. All experiments were performed with a 10-90 mixture at a total gas pressure of 133 Pa. The meaning of the symbols is as in Table I.

Buffer gas	T (K)	ΔP_m (mW)	Γ/kv_0	Δ_0 (units of 10^{-2})	Δ_1 (units of 10^{-2})
Ne	293	84	0.25	0.52	−0.9
	420	42	0.25	0.50	−0.8
Ar	293	81	0.30	0.65	−3.4
	415	34	0.30	0.60	−2.4
Kr	293	92	0.32	0.71	−5.7
Xe	293	95	0.35	−0.49	−4.9

For the buffer gas Ar, anomalous LID was observed. The induced concentration difference corresponds to a $(\Delta\nu/\nu)_{\text{eff}}$ having a substantial velocity dependence, as expressed by the large value of Δ_1 [see Table II and Fig. 6(b)]. The outer extrema become more pronounced when the temperature is raised to ≈400 K. The data for the various temperatures were found to coincide well.

For the buffer gases Kr and Xe at 293 K, a rather normal dispersionlike signal for Δx_a was observed. The $(\Delta\nu/\nu)_{\text{eff}}$ is negative and strongly velocity dependent [see Fig. 6(b)]. The fit parameters are given in Table II.

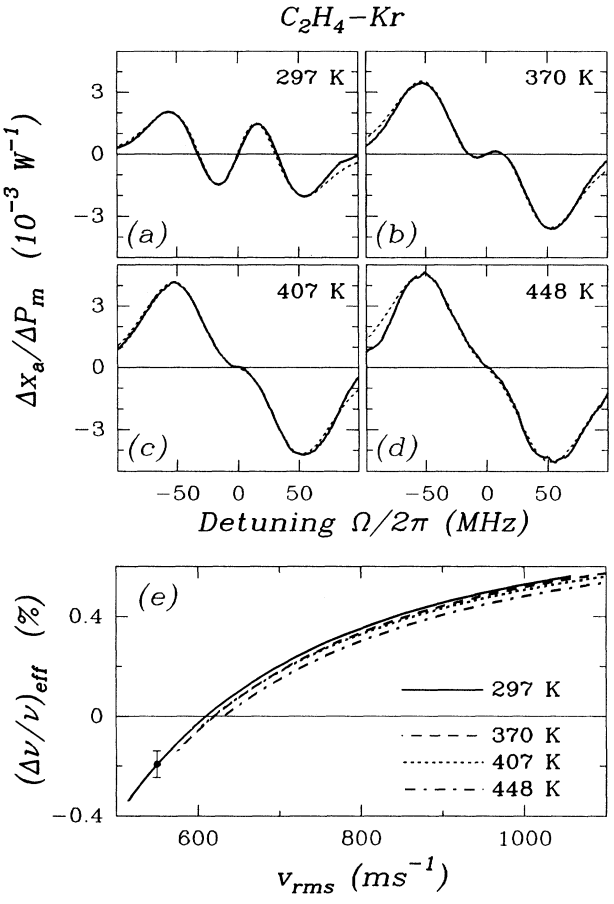

FIG. 4. Experimental results (solid lines) for a C_2H_4-Kr mixture at various temperatures [(a)–(d)]. The concentration difference Δx_a is normalized to the absorbed laser power at line center, ΔP_m, to correct for the trivial temperature dependence of the fraction of excited particles (see text). The fit of Eq. (16) is shown by the dotted line. In (e), the effective relative difference in collision frequency, $(\Delta\nu/\nu)_{\text{eff}}$, is shown, as calculated from the LID profiles (a)–(d) as a function of the average relative velocity v_{rms}. Relevant details are in Table I. The error bar refers to the estimated error in $(\Delta\nu/\nu)_{\text{eff}}$ for the low- and intermediate-velocity range (see text).

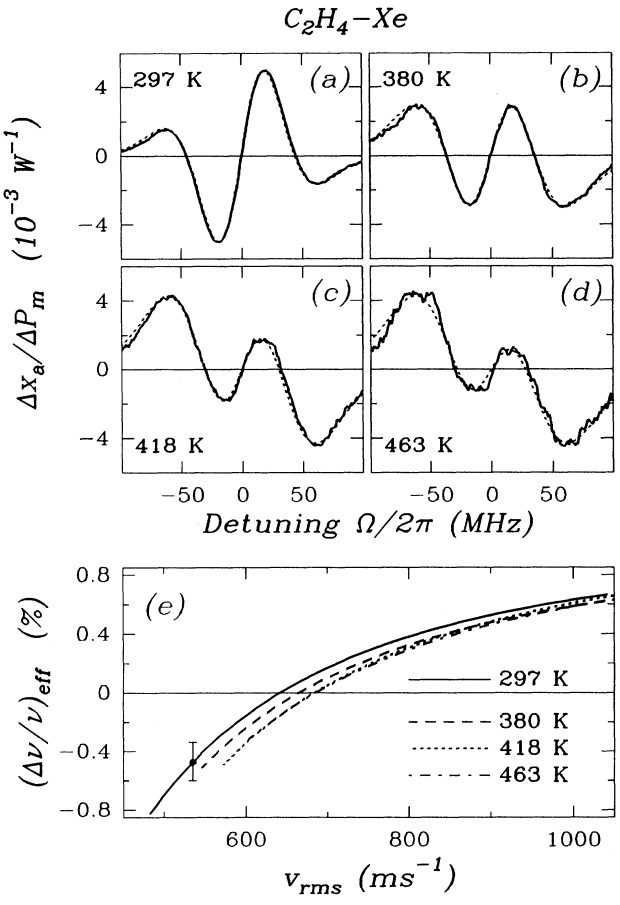

FIG. 5. Experimental results (solid line) and their fit (dotted line) for a C_2H_4-Xe mixture at various temperatures [(a)–(d)]. The concentration difference Δx_a is normalized to the absorbed laser power at line center, ΔP_m, to correct for the trivial temperature dependence of the fraction of excited particles (see text). In (e), $(\Delta\nu/\nu)_{\text{eff}}$ is calculated as a function of v_{rms}. Relevant details are in Table I. The error bar refers to the estimated error in $(\Delta\nu/\nu)_{\text{eff}}$ for the low- and intermediate-velocity range (see text).

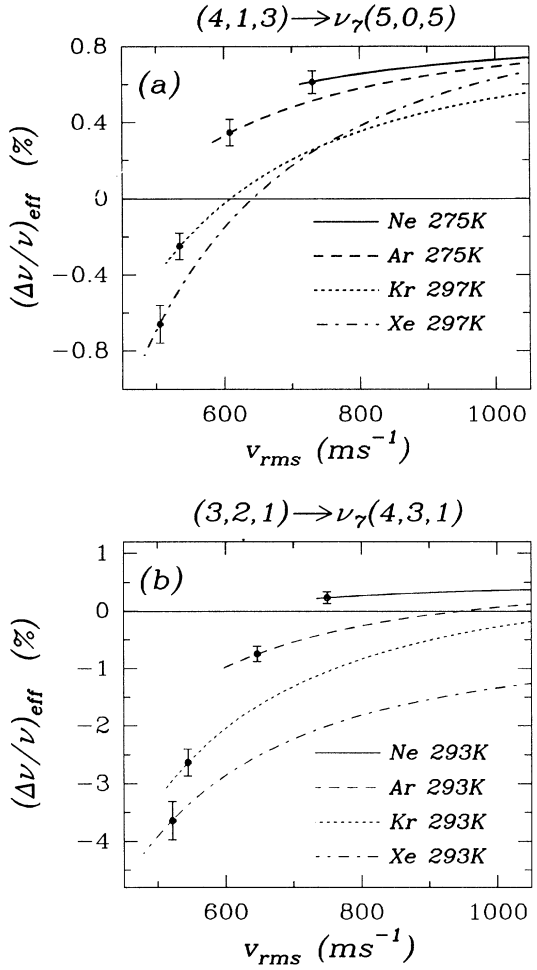

FIG. 6. The results for $(\Delta\nu/\nu)_{\text{eff}}$ as a function of rms relative velocity v_{rms} for the buffer gases Ne, Ar, Kr, and Xe. (a) pertains to the data for the (5,0,5)→ν_7(4,1,3) transition, which were already shown in Figs. 2–5. (b) pertains to the data for the (3,2,1)→ν_7(4,3,1) transition. Note the differences in vertical scale. The error bars given refer to the low- and intermediate-velocity range (see text).

IV. DISCUSSION AND CONCLUSIONS

As shown in Sec. III, the data on the (4,1,3)→ν_7(5,0,5) and (3,2,1)→ν_7(4,3,1) transition exhibit the same trends. Since most data were obtained for the first transition, we will restrict the discussion to this one; the same conclusions may be drawn from the data for the (3,2,1)→ν_7(4,3,1) transition.

First, we observed that anomalous LID can be accurately described by our ansatz (11) for the dependence of $(\Delta\nu/\nu)_{\text{eff}}$ on the laser detuning. As was shown in Figs. (2)–(5), a good description of the LID signals for ethylene in the noble gases was obtained by including only two terms in the expansion of $(\Delta\nu/\nu)_{\text{eff}}$. It should be noted, however, that the anomalous LID signals can also be described using other expansions than ansatz (11). We found following Ref. [10] that the expansion

$$(\Delta\nu/\nu)_{\text{eff}}=\sum_m \tilde{\Delta}_m (v_x/v_0)^{2m}$$

can give a good description of anomalous LID too when enough terms are included [10]. But it turned out that the high-velocity part of $(\Delta\nu/\nu)_{\text{eff}}$ especially is very sensitive to the type of expansion. This can be understood from Eq. (8). For large detuning, the Maxwell factor $W(\mathbf{v})$ in the excitation probability $p(\mathbf{v})$ [see Eq. (5)] fully suppresses the rhs of Eq. (8). As a result, the distinction between the experimental curve (Δx_a) and the fit becomes insensitive to the type of expansion for $(\Delta\nu/\nu)_{\text{eff}}$. This therefore yields relatively large error bars in $(\Delta\nu/\nu)_{\text{eff}}$ for large average relative velocities. Our expansion for $(\Delta\nu/\nu)_{\text{eff}}$ has no such disadvantages for high v_{xL}. It has to be noticed, however, that both expansions for $(\Delta\nu/\nu)_{\text{eff}}$ have the disadvantage that the resulting functions $\varphi_m(\Omega)$ are not orthogonal. This makes it difficult to find a unique set of coefficients Δ_m.

From the temperature dependence of the LID signal, conclusions can be deduced on the dependence of $(\Delta\nu/\nu)_{\text{eff}}$ on the real *relative* velocity between two particles. In Figs. 4 and 5 we observe that $(\Delta\nu/\nu)_{\text{eff}}$ is a unique monotonic function of the average relative velocity v_{rms} and that for a particular buffer gas, $(\Delta\nu/\nu)_{\text{eff}}$ as a function of v_{rms} varies marginally with temperature (i.e., for a particular value of v_{rms}, $(\Delta\nu/\nu)_{\text{eff}}$ is independent of temperature). Yet, v_{rms} samples over a wider range of real relative velocities at higher temperatures, where the Maxwellian is wider [see Eq. (9)]. This must mean that $(\Delta\nu/\nu)_{\text{eff}}$ is a smoothly varying function of the real *relative* velocity between two collision partners.

The dependence of the observed concentration difference on the buffer gas can only partially be attributed to the mass dependence of the average relative velocity. For an identical interaction potential between the C_2H_4 molecule and the various noble-gas atoms, we expect the curves in Fig. 6 to coincide. This however, is not observed in Fig. 6. Thus, the interaction potential plays an important role.

Actually, the fit parameters Δ_0 and Δ_1 can be used to deduce information on the role of the intermolecular potential in $(\Delta\nu/\nu)_{\text{eff}}$. The parameter Δ_0 is found to be temperature independent as it is supposed to be according to ansatz (11). For large relative velocities, where only Δ_0 survives, the repulsive part of the interaction potential should dominate and the molecule should behave as a hard sphere. Upon decreasing the average relative velocity, the attractive part of the potential begins to play an appreciable role. This suggests that $\Delta_1(v_0/v_{\text{rms}})^2$ is related to the attractive part of the potential. Upon increasing the noble-gas mass, the attractive part of the potential increases (this was shown for C_2H_4-Ne and C_2H_4-Ar complexes by Hutson, Clary, and Beswick [17]). A heavier noble gas therefore favors the Δ_1 term, which is indeed observed in Fig. 6. This suggests that the attractive part of the intermolecular potential is essential for the occurrence of anomalous LID.

Finally, we observed that Δ_0 and Δ_1 depend strongly

on the transition under study (see Tables I and II). This is consistent with the splitting described by Eq. (2).

Data on $(\Delta\nu/\nu)_{\text{eff}}$ like those shown in Fig. 6 may be compared with model calculations of the interaction potential for rovibrationally excited C_2H_4 interacting with noble-gas atoms. For the systems presented here, such calculations are not yet available. For simpler systems like HF-Ar, such calculations are being performed [18]. Measurements on such systems are under way [19].

ACKNOWLEDGMENTS

The authors would like to thank I. Kuščer, A.M. Shalagin, G. Nienhuis, L. A. Viehland, and H. I. Bloemink for fruitful discussions. The work is part of the research program of the Foundation for Fundamental Research on Matter (FOM) and was made possible by financial support from the Netherlands Organization for Scientific Research (NWO).

*Permanent address: Institute of Automation and Electrometry, 630090 Novosibirsk, Russia.

[1] F. Kh. Gel'mukhanov and A. M. Shalagin, Pis'ma Zh. Eksp. Teor. Fiz. **29**, 773 (1979) [JETP Lett. **29**, 711 (1979)].

[2] For a review on atomic LID, see E. R. Eliel, Adv. At. Mol. Opt. Phys. (to be published).

[3] For a review on molecular LID, see L. J. F. Hermans, Int. Rev. Phys. Chem. **11**, 289 (1992).

[4] G. J. van der Meer, H. I. Bloemink, E. R. Eliel, and L. J. F. Hermans, J. Mol. Spectrosc. **153**, 419 (1992).

[5] V. R. Mironenko and A. M. Shalagin, Izv. Akad. Nauk. SSSR, Ser. Fiz. **45**, 995 (1981) [Bull. Acad. Sci. USSR, Phys. Ser. **45**, 87 (1981)].

[6] G. J. van der Meer, J. Smeets, S. P. Pod'yachev, and L. J. F. Hermans, Phys. Rev. A **45**, 1303 (1992).

[7] C. H. Townes and A. L. Schawlow, *Microwave Spectroscopy* (Dover, New York, 1975).

[8] P. L. Chapovsky, G. J. van der Meer, J. Smeets, and L. J. F. Hermans, Phys. Rev. A **45**, 8011 (1992).

[9] F. Kh. Gel'mukhanov and A. I. Parkhomenko, Phys. Lett. A **162**, 45 (1992).

[10] P. L. Chapovsky, L. J. F. Hermans, G. J. van der Meer, and A. M. Shalagin, (unpublished).

[11] The coefficients $\Delta_0, \Delta_1, \ldots$ may be temperature dependent. Only when the LID signal is invariant with respect to v_x^2/T, will the coefficient Δ_1 be temperature independent.

[12] G. J. van der Meer, R. W. M. Hoogeveen, L. J. F. Hermans, and P. L. Chapovsky, Phys. Rev. A **39**, 5237 (1989).

[13] *Handbook of Mathematical Functions* edited by M. Abramowitz and I. A. Stegun (Dover, New York, 1964).

[14] Since heating of the windows of the capillary has to be avoided, a small temperature inhomogeneity over the last 5 mm of the channel arises. To investigate the effect of this gradient, the temperature given by the thermocouples was compared with the temperature derived from the width of the absorption profile of a low-pressure gas at low laser intensity (which is essentially only Doppler broadened). The temperatures agreed within a few percent and thus we assume that the temperature inhomogeneity has negligible influence on the experimental data.

[15] F. Herlemont, M. Lyszyk, J. Lemaire, C. Lambeau, M. Vleeschouwer, and A. Fayt, J. Mol. Spectrosc. **94**, 309 (1982).

[16] The experiments for C_2H_4 in Kr and Xe were performed at reduced gas pressure to minimize the response time of the system, which is inversely proportional to the diffusion coefficient (and thus proportional to the pressure). This should not have a significant effect on the results: As discussed previously in Ref. [6], the anomalous signals are only weakly dependent on the laser power, the total gas pressure, and the mole fraction x_a in the range $\Gamma/kv_0 = 0.3-0.5$.

[17] J. M. Hutson, D. C. Clary, and J. A. Beswick, J. Chem. Phys. **81**, 4474 (1984).

[18] J. M. Hutson, J. Chem. Phys. **96**, 6752 (1992).

[19] E. J. van Duyn, H. I. Bloemink, E. R. Eliel, and L. J. F. Hermans (private communication).